Korean J. Chem. Eng., **27**(4), 1338-1342 (2010)
DOI: 10.1007/s11814-010-0200-0

Preparation and characteristics of nano-B_4C/PVA particles and ultra high molecular weight polyethylene composites

Young Rang Uhm, Jaewoo Kim†, Jinwoo Jung, and Chang Kyu Rhee

Nuclear Materials Research Division, Korea Atomic Energy Research Institute,
1045 Daedukdaero, Daejeon 305-353, Korea
(*Received 28 September 2009 • accepted 16 December 2009*)

Abstract−In-situ mechanical process for preparation of the polyvinyl alcohol (PVA) coated nano-B_4C powder was investigated by using a high-energy ball mill. The produced PVA coat on the surface of nano-B_4C particles was observed by x-ray diffraction (XRD) and confirmed by TEM images. The average particle size of the produced nano-B_4C/PVA particles was in the range of several tens to hundreds of nanometers depending on the milling conditions. The polymer composites were fabricated by hot pressing ultra high molecular weight polyethylene (UHMWPE) powder mixed with nano-B_4C/PAV and micro-B_4C powders, respectively. Nano-B_4C/PVA dispersed UHMWPE shows slightly lower crystallinity and stiffness than micro-B_4C dispersed UHMWPE based on differential scanning calorimetry (DSC) and dynamic mechanical analysis (DMA) evaluations.

Key words: PVA, B_4C, Ball Mill, Nano Powder, Polymer Nanocomposite

INTRODUCTION

Researches on ceramic/polymer nanocomposites have been growing exponentially during the last decades due to their structures and properties which are useful for designing advanced engineering materials. Those ceramic/polymer nanocomposites show in general higher mechanical, thermal, electrical, and optical properties compared to pure polymeric materials [1-3]. For example, thermal, electric, and environmental resistive properties of high density polyethylene (HDPE) could be enhanced by dispersing the ceramic nano-fillers in HDPE. Polyethylene incorporated with ceramic nano-fillers such as SiO_2, Al_2O_3, and $CaCO_3$, etc. has been widely explored in this regard [4-7]. Among various ceramic materials, B_4C is one of the most promising structural materials due to its melting point (2,427 °C) and the Vickers hardness (>30 GPa) [8]. The B_4C/ HDPE composite is also useful for shielding neutrons in extreme radiation environments such as nuclear reactors, space shuttles, satellites, and military armors, etc. because of its superior high energy neutron attenuating and thermal neutron absorbing behaviors due to high concentrations of hydrogen and boron (thermal neutron absorption cross-section of boron ~760 barn, barn=10^{-24} cm^2), respectively [9,10]. However, there is little information available related to preparations of this type of material. Recently, it was reported that the neutron shielding efficiency could be enhanced by using the smaller B_2O_3 filler dispersed polyvinyl alcohol (PVA) [11]. Theoretical estimation for filler size-dependent thermal neutron diffusion without absorption in nano-structural material was also reported [12]. Preparations of such materials are difficult because of the agglomeration of the nanoparticles in the polymer matrix due to high surface energy of the nanoparticles. Surface treatment of the nanoparticles to enhance the wettability with the polymeric matrix is therefore necessary to inhibit or minimize the agglomeration of the nanoparticles. Most surface treatments of the nanoparticles involve the stepwise solution process and also require complicated chemistry [2,13-15], whereas mechanical surface modification is a simple and dried process using a mixer or a ball mill [16,17]. Ball milling has been used for preparations of either various nanoparticles or surface coated nanocomposites [17-26]. Theoretical evaluations using the energy transfer between the balls and materials have been also reported [27-30]. The present investigation is focused on pulverization of micro-sized B_4C powder as well as PVA coating on the B_4C particles. Prepared nano-B_4C/PVA and micro-B_4C powders were mixed with ultra high molecular weight polyethylene (UHMWPE) powder, respectively, then hot pressed to fabricate the polymer composite sheets. Various analytic tools were used to evaluate the thermo-physical characteristics of the prepared nano-B_4C/PVA particles and polymer composites.

EXPERIMENTAL

B_4C (average particle size of ~5 μm, purity >99.9%, Kojundo) and PVA (molecular weight of 50,000, purity >99.9%, Aldrich) powders were used as raw materials. A high-energy ball mill (Pulverisette 6, Fritsch) with two stainless steel (STS) jars with the volume of 133 cm^3 was used for milling. The milling temperature was maintained lower than 60 °C by tap water cooling. The jars were sealed with a rubber O-ring and operated at 1 atm of the air. The weight ratio between B_4C and PVA was 1 : 1, while the ball to powder weight ratio was 10 : 1. STS balls with 6 mm diameter were used. Rotation speeds of the disk were varied from 400 to 800 rpm depending on the milling conditions. Prepared nano-B_4C/PVA and micro-B_4C powders were mixed with UHMWPE (Ticona GUR) powder by using a powder mixer, respectively, prior to preparation of the polymer composites. The nano-B_4C/PVA and micro-B_4C dispersed UHMWPE sheets (thickness ~30 mm) were then fabricated by hot pressing at 190 °C and 20 MPa for 20 min, respectively. The

†To whom correspondence should be addressed.
E-mail: kimj@kaeri.re.kr

characteristics of the prepared samples in each step were evaluated by using various analytic tools, including the particle size analyzer (PSA), X-ray diffraction (XRD), scanning electron microscope (SEM), and transmission electron microscope (TEM). The thermo-physical characteristics of the nano- and micro-B_4C particle dispersed UHMWPE sheets were also analyzed by means of differential scanning calorimetry (DSC) and dynamic mechanical analysis (DMA).

EXPERIMENTAL RESULTS

1. Characteristics of Nano-B_4C/PVA Powder

To produce the nano-sized B_4C particles, micro-sized B_4C premixed with PVA powder was pulverized in a high energy ball mill. Prior to pulverization of powders, the amount of transferred energy from the balls to powder by collisions was estimated based on the model introduced by Magini et al. [28]. For the STS and ZrO_2 (zirconia) balls, $\Delta E/Q_{max}=(4.43\times10^4)\, d_b\, \omega_p^{1.2}/\sigma$, where ΔE is the transferred energy, Q_{max} is the maximum quantity of trapped material on the surface of a ball, d_b is the diameter of a ball, ω_p is the rotation speed of the disk, and σ is the surface density of powder on a ball, is plotted in Fig. 1. Both STS and zirconia balls show similar pattern of energy transfer per unit mass, while the STS balls show slightly higher energy transfer than the zirconia balls. Based on this estimation, the STS ball was chosen for the experiments. Fig. 1 also shows the milling energy dependent particle size reduction during initial 10 min of pulverization. The average particle size decreases as the disk rpm increases, i.e., milling energy increases, as expected. The average size of bare nano-B_4C was measured by PSA (90Plus, Brookhaven Instruments Corp). Prior to particle size measurement, the PVA coat on the surface of B_4C was dissolved in distilled water and ultrasonificated for 10 min to prevent the agglomeration between the particles. Although PSA measurements produce multimodal size distributions, which indicates some particles are not fully pulverized, the average particle size obtained from the unimodal distribution shows the trends of size reduction produced from the milling process even though it is broadened.

Degrees of pulverization for the B_4C particles from ~5 μm (raw powder) to ~50 nm depending on the milling time are shown in Fig. 2. Milling was performed with and without PVA at 700 rpm to compare the effect of the polymeric surfactant. The average size of the B_4C particles was decreased steeply at the initial stage of pulverization from ~5 μm to ~600 nm for both cases. However, further size reduction was not efficient when pulverized without PVA, while the size was decreased efficiently to below 100 nm when pulverized with PVA. This indicates that the re-aggregation of the B_4C particles without PVA might be more severe than that with PVA under the same experimental conditions. Also, the milling energy for crushing powder should overcome the potential energy of aggregation between B_4C particles. It was reported that the preparation of

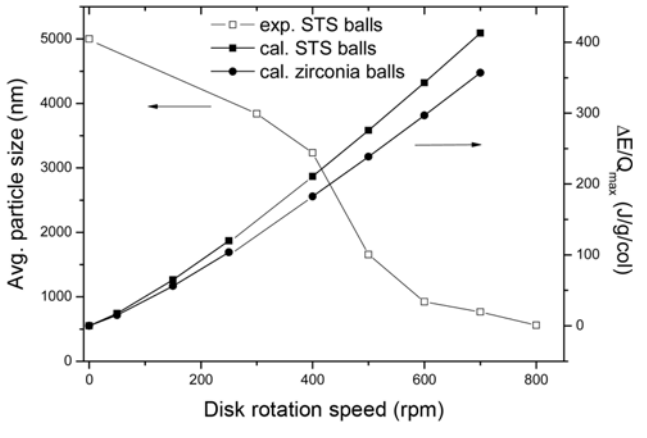

Fig. 1. Average B_4C particle size dependent on the milling energy and the estimations of transferred energy, $\Delta E/Q_{max}$, for the STS and ZrO_2 balls.

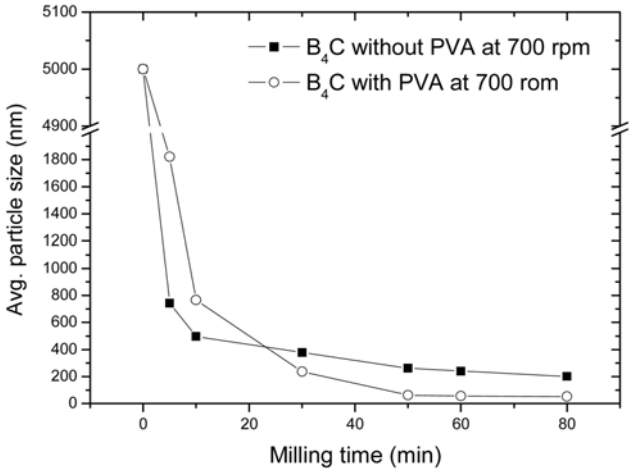

Fig. 2. Decrease of the average size of B_4C dependent on milling time at 700 rpm with and without PVA.

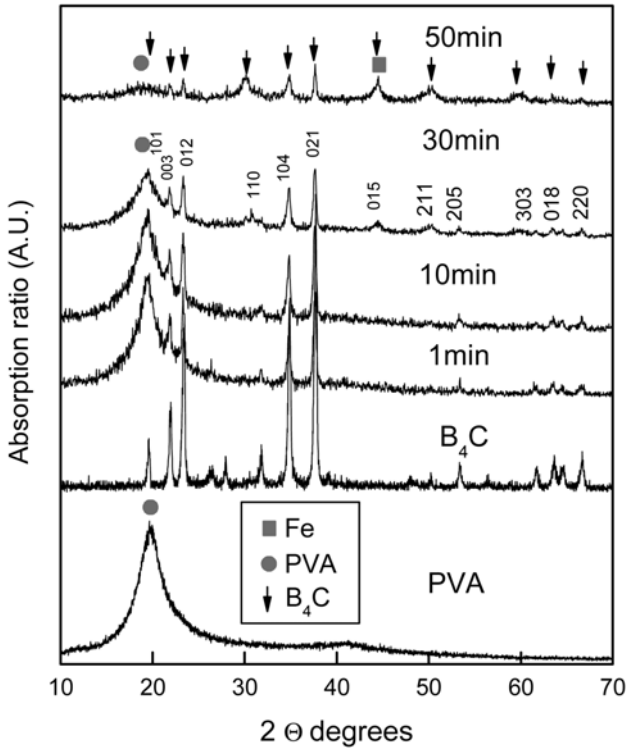

Fig. 3. X-ray diffraction patterns for pure PVA, B_4C, and nano-B_4C/PVA composites for various milling time.

nano-B_4C powder by the mechanical milling process without surfactants requires extremely long milling time longer than ~100 h at 200 rpm to produce ~300 nm B_4C particles [18,19]. However, B_4C with the surfactant could be crushed more efficiently to nano-scale if a high energy ball mill is used. It is clear that milling of B_4C together with the surfactant can enhance the pulverization efficiency, while the surface of the particles can be coated simultaneously with the polymeric agent which can enhance the wettability of the nanoparticles in the polymeric matrix.

PVA coat on the surface of the B_4C nanoparticles was observed by the x-ray diffraction (D/MAX-3C, Rigaku) spectrum. The x-ray diffraction patterns of pure PVA, pure B_4C, and the B_4C particles covered with PVA milled at 700 rpm for different milling time are shown in Fig. 3. The peak heights for PVA decrease as the milling time increases, and the peaks are finally disappeared for powder milled for 50 min. This means that the amorphous phase of PVA on the B_4C surface was generated from the semi-crystalline structured initial PVA. The Fe impurity was also observed for milled nano-B_4C/PVA powder, which was produced during the milling process as expected. Consequently, the in-situ approach we explored in this investigation efficiently produced the finer nanoparticles during a short period of time and also coated the surface of the nanoparticles using a polymeric surfactant simultaneously. In addition to the x-ray diffraction patterns, PVA coat on the B_4C nanoparticles was also confirmed by TEM images. Fig. 4(a)-(d) shows the TEM (JEM-2100F, JEOL Ltd. Japan) morphologies of the nano-B_4C/PVA particles milled at 700 rpm for 50 min. The shapes of most of the crushed particles are spherical-like and coated with PVA (Fig. 4(d)). The images also show some particles are constituted with the smaller particles of several tens of nanometers. This means that some aggregations of the nanoparticles are inevitable for this type of milling process. However, it might be useful to produce the nanosized B_4C particles coated with PVA without any aqueous agent or complicated chemistry. In the in-situ coating process, the surfactant particles can be trapped between the colliding balls experiencing plastic deformation and flattening to be coated on the surface of the host particles. Such flattened surfactant particles adhere with the host particles so that they can coat the surface of the host particles forming a film.

2. Morphologies of B_4C-UHMWPE Composites

The as-prepared nano-B_4C/PVA composites and micro-B_4C with 1.5 and 5.0 wt% were mixed with UHMWPE powder and the sheets were fabricated by hot pressing, respectively. A powder mixer was used for homogeneous blending of the filler and polymer powders. Fig. 5 shows the SEM (Sirion, FEI Netherlands) micrographs of 5.0 wt% (a) micro-B_4C dispersed UHMWPE and (b) the nano-B_4C/PVA dispersed UHMWPE, respectively. As shown in Fig. 5(a), the size of micro-B_4C is ~5 μm, which is the same as the starting raw particles. This indicates that the agglomeration between the particles for hot pressing is not serious from a dispersion standpoint. However, the adhesion of the particles with the polymer matrix looks poor presumably because no surfactant was applied for the micro-B_4C particles prior to fabrication. On the other hand, the image (Fig. 5(b)) of the nano-B_4C dispersed UHMWPE samples shows the homo-

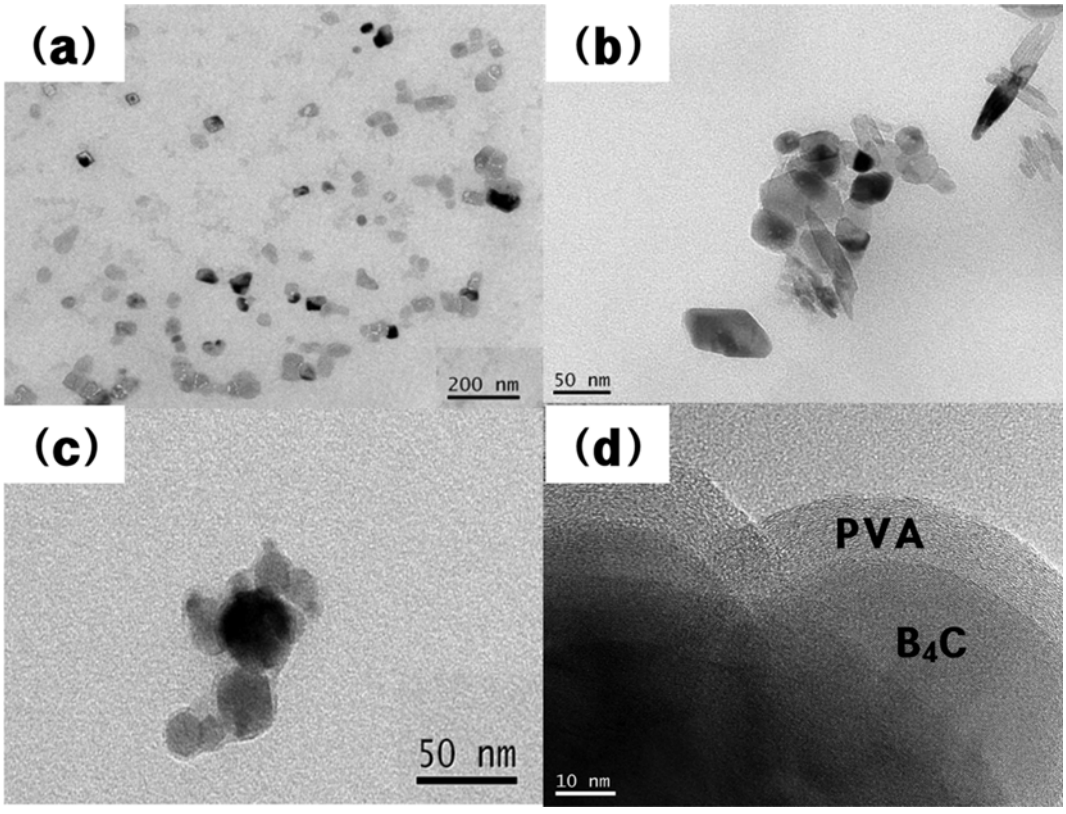

Fig. 4. TEM morphologies of the nano-B_4C/PVA composites milled at 700 rpm for 50 min; (a) distribution of nanocomposites, (b), (c) typical shapes of the nanocomposite, (d) shape of surface coat on the nanocomposite.

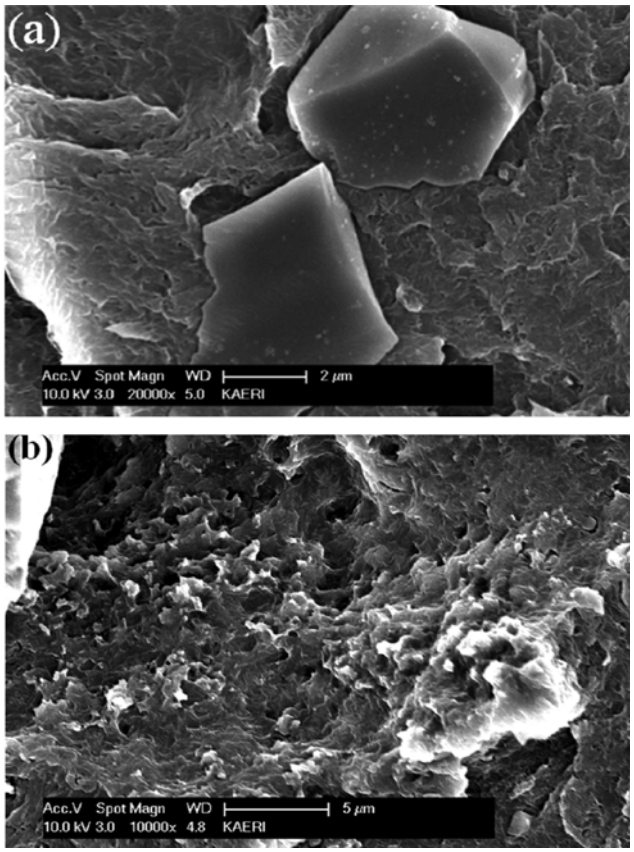

Fig. 5. SEM morphologies for 5.0 wt% (a) micro-B_4C and (b) nano-B_4C particles dispersed UHMWPE sheet fabricated by powder hot pressing.

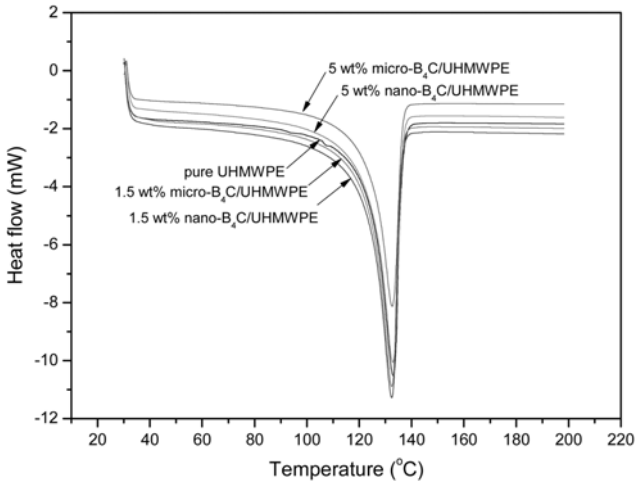

Fig. 6. DSC curves for pure UHMWPE, micro-B_4C dispersed UHMWPE, and nano-B_4C dispersed UHMWPE.

Table 1. DSC thermal parameters for pure UHMWPE, micro-B_4C/UHMWPE, and nano-B_4C/UHMWPE composites

Materials	T_m (°C)	ΔH_m (J/g)	X_c
pure UHMWPE	132.79	101.90	35.38
micro-B_4C/UHMWPE (1.5 wt%)	132.62	102.18	35.48
nano-B_4C/UHMWPE (1.5 wt%)	132.53	95.94	33.31
micro-B_4C/UHMWPE (5.0 wt%)	131.84	96.53	33.52
nano-B_4C/UHMWPE (5.0 wt%)	131.98	94.42	32.78

geneously dispersed nanometric particles as well as good adhesion of the particles with the polymer matrix. Adhesion of the particles with the polymeric matrix is very important to enhance the thermo-mechanical properties of the polymer composites. If adhesion of the inorganic fillers with the polymeric matrix is not good, the properties of the polymer composites could be deteriorated compared to those for pure polymer.

3. Thermo-mechanical Properties of B_4C-UHMWPE Composites

By using the endothermic heating process of the prepared polymer composites, thermal characteristics were evaluated by means of DSC (DSC-Q100, TA Instrument) analyses. Parameters including the melting temperature (T_m), the enthalpy of fusion (ΔH_m), and the degree of crystallinity (X_c) of the UHMWPE composites were obtained from the DSC curves in Fig. 6 and are listed in Table 1. The degree of crystallinity X_c of the UHMWPE composites compared to pure UHMWPE can be calculated by using the relation $X_c=\Delta H_m(T_m)/\Delta H_m^o(T^om)$, where $\Delta H_m(T_m)$ is the enthalpy of fusion at T_m for the UHMWPE composite and $\Delta H_m^o(T^om)$ is the enthalpy of fusion at equilibrium melting temperature T_m^o for pure UHMWPE [29]. According to Fig. 6 and Table 1, melting points for most polymer composites including pure UHMWPE are about the same at ~132 °C. Similar melting points between the samples might be due to maintained flexibility of the polymer chains even for the B_4C fillers dispersed in the medium. Similar results were also observed for the nanosized calcium carbonate dispersed HDPE composite [7]. However, enthalpy of fusion for 5.0 wt% nano-B_4C dispersed UHMWPE is the lowest, while 1.5 wt% micro-B_4C dispersed UHMWPE show the highest same as pure UHMWPE. This means that addition of B_4C in UHMWPE decreases the crystallinity of the composites compared to pure UHMWPE. It is assumed that the filler particles decrease the mobility of the UHMWPE chains for producing crystalline structure [32,33]. As a result, the degree of crystallinity decreases as the filler contents increase and filler size decreases. It is also assumed that the good adherence of the smaller particles with the polymer matrix contributes to lower mobility of the polymer chains.

The dynamic mechanical properties of pure UHMWPE, micro-B_4C dispersed UHMWPE, and nano-B_4C dispersed UHMWPE composites were also evaluated by means of DMA (Q800, TA Instruments) in the temperature range 40 to 180 °C and the heating rate of 10 °C/min using the samples whose size was 35 mm×10 mm×1.5 mm. Fig. 7 shows the storage modulus and tanδ for 1.5 wt% nano-, and micro-B_4C dispersed UHMWPE composites and pure UHMWPE. The storage modulus for pure UHMWPE is higher than those for B_4C dispersed UHMWPE composites, while the storage modulus for micro-B_4C dispersed UHMWPE is slightly higher than that for nano-B_4C dispersed UHMWPE. This means that the stiffness for pure UHMWPE could be decreased by addition of B_4C fillers, especially by adding nano-B_4C at lower temperature region. This is somewhat different from the other result increasing the stiffness by adding ceramic fillers in polymer [5]. This might be due to

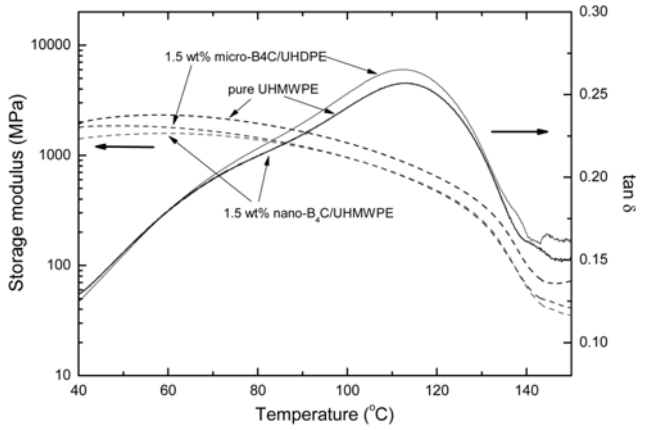

Fig. 7. Storage modulus and tanδ curves for pure UHMWPE, 1.5 wt% micro-B_4C/UHMWPE, and 1.5 wt% nano-B_4C/UHMWPE.

interruption of the long polymer backbones and chains in the UHMWPE matrix by the ceramic impurities causing lower load transfer in polymer.

CONCLUSION

The present investigation is focused on the in-situ pulverization of micro-sized B_4C powder and dry coating of the B_4C particles using polymeric surfactant PVA for modification of the particle surface properties and/or functionality. This type of one-step dry coating method does not involve any complicated chemistry and multi-step solution processes such as micro-emulsion and sol-gel, etc. The average particle size of the produced nano-B_4C/PVA particles was in the range of several tens to hundreds of nanometers depending on the milling conditions. PVA layer on the surface of nanoparticles was confirmed by XRD spectrum and TEM images. The degree of crystallinity decreased as the B_4C filler content increased and the size of the B_4C particles decreased. By dispersing B_4C fillers, stiffness of UHMWPE was decreased. Consequently, in-situ pulverization and surface treatment process developed in this investigation can be applied for production of the surface-coated nanoparticles, while enhancement of the thermo-mechanical properties of the UHMWPE composites requires more researches in depth.

ACKNOWLEDGEMENT

This work was supported by the Nuclear Energy R&D Program (Grant No. R-2007-3-155) operated by the Ministry of Knowledge Economy in the Republic of Korea.

REFERENCES

1. M. Alexandre and P. Dubois, *Mat. Sci. Eng. R.*, **28**, 1 (2000).
2. B. A. Rozenberg and R. Tenne, *Prog. Polym. Sci.*, **33**, 40 (2008).
3. A. P. Kumar, D. Depan, N. S. Tomer and R. P. Singh, *Prog. Polym. Sci.*, In press.
4. N. Garcia, M. Hoyos, J. Guzman and P. Tiemblo, *Polym. Degrad. Stabil.*, **94**, 34 (2009).
5. K. Chrissafis, K. M. Paraskevopoulos, E. Pavlidou and D. Bikiaris, *Thermochim. Acta*, **485**, 65 (2009).
6. Q. Jiasheng and H. Pingsheng, *J. Mater. Sci.*, **38**, 2299 (2003).
7. S. Sahebian, S. M. Zebarjad, J. V. Khaki and S. A. Sajjadi, *J. Mater. Process. Tech.*, **209**, 1310 (2009).
8. F. Thevenot, *J. Eur. Ceram. Soc.*, **6**, 205 (1990).
9. C. Harrison, E. Burgett, N. Hertel and E. Grulke, *Ceramic Eng. Sci. Proc.*, **29**(8), 77 (2009).
10. T. Yasin and M. N. Khan, *e-Polymers*, **059**, 1 (2008).
11. J. Kim, Y. R. Uhm, M.-K. Lee, H. M. Lee and C. K. Rhee, *Trans. Kor. Nuc. Soc.*, 641 (2008).
12. V. A. Artem'ev, *Atom. Energy*, **94**(4), 282 (2003).
13. E. Glogowski, R. Tangirala, T. P. Russel and T. Emrick, *J. Polym. Sci. Part A: Polym.Chem.*, **44**, 5076 (2006).
14. K. H. Yoon, S. B. Park and B. D. Yang, *Mater. Chem. Phys.*, **87**, 39 (2004).
15. R. Palkovits, H. Althues, A. Rumplecker, B. Tesche, A. Dreier and U. Holle, *Langmuir*, **21**, 6048 (2005).
16. Y. Ouabbas, A. Chamayou, L. Galet, M. Baron, G. Thomas, P. Grosseau and B. Guilhot, *Powder Technol.*, **290**, 200 (2009).
17. J. Kim, M. Satoh and T. Iwasaki, *Mat. Sci. Eng.*, **A342**, 258 (2003).
18. F. Deng, H.-Y. Xie and L. Wang, *Mater. Lett.*, **60**, 1771 (2006).
19. M. W. Mortensen, P. G. Sørensen, O. Björkdahl, M. R. Jensen, H. J. G. Gundersen and T. Bjørnholm, *Appl. Radiat. Isotopes*, **64**, 315 (2006).
20. M. A. Bab, L. Mendoza-Zelis and L. C. Damonte, *Acta Mater.*, **49**, 4205 (2001).
21. S. Sheibani, A. Ataie, S. Heshmati-Maneshe and G. R. Khayati, *Mater. Lett.*, **61**, 3204 (2007).
22. S. Coste, G. Bertrand, C. Coddet, E. Gaffet, H. Hahn and H. Sieger, *J. Alloy Compd.*, **434-435**, 489 (2007).
23. J. Lee, Q. Zhang and F. Saito, *Ind. Eng. Chem. Res.*, **40**, 4785 (2001).
24. A. I. Gusev and A. S. Kurlov, *Nanotechnology*, **19**, 1 (2008).
25. J. D. Tucker, P. L. Lear, G. S. Atkinson, S. Lee and S. J. Lee, *Korean J. Chem. Eng.*, **17**(5), 506 (2000).
26. H. K. Choi and W. S. Choi, *Korean J. Chem. Eng.*, **20**(4), 783 (2003).
27. K. S. Venkataraman and K. S. Narayanan, *Powder Technol.*, **96**, 190 (1998).
28. M. Magini, A. Iasonna and F. Padella, *Scripta Mater.*, **34**(1), 13 (1996).
29. H. Zhang and X. Liu, *Int. J. Refract. Met. H.*, **19**, 203 (2001).
30. J. M. Castillo, R. Lapasin and M. Grassi, *Ind. Eng. Chem. Res.*, **42**, 2015 (2003).
31. Y. Kong and J. N. Hay, *Polymer*, **42**, 3873 (2002).
32. W. Zhou, S. Qi, H. Li and S. Shao, *Thermochim. Acta*, **452**, 36 (2007).
33. W. Zhou, D. Yu, C. Min, Y. Fu and X. Guo, *J. Appl. Polym. Sci.*, **112**, 1695 (2009).